

# Inertia Estimation through Covariance Matrix

Federico Bizzarri, *IEEE Senior Member*, Davide del Giudice, *IEEE Student Member*, Samuele Grillo, *IEEE Senior Member*, Daniele Linaro, *IEEE Member*, Angelo Brambilla, *IEEE Member*, and Federico Milano, *IEEE Fellow*

**Abstract**—This work presents a technique to estimate on-line the inertia of a power system based on environment measurements. The proposed approach utilizes the covariance matrix of these measurements and solves an optimization problem that fits such measurements to the synchronous machine classical model. We show that the proposed technique is adequate to accurately estimate the actual inertia of synchronous machines and also the virtual inertia provided by the controllers of converter-interfaced generators that emulate the behavior of synchronous machines. We also show that the proposed approach is able to estimate the damping of the machines. This feature is exploited to estimate the droop of grid-following converters. The technique is comprehensively tested on a modified version of the IEEE 39-bus system.

**Index Terms**—Inertia estimation, stochastic differential equations, covariance matrix.

## I. INTRODUCTION

### A. Motivation

The inertia constant has become a volatile parameter in power systems with high penetration of renewable and non-synchronous resources [1]. The estimation of the available inertia, on the other hand, is a valuable information that can help system operators to ensure the security of the grid [2]. This paper addresses this problem and aims at developing an on-line inertia estimation method based on ambient measurements and their stochastic behavior.

### B. Literature Review

There are mainly two methods for the on-line estimation of the inertia available in a power system: (i) methods based on the measurement of frequency and power variations after a disturbance or by injecting a probing signal and (ii) methods that utilize ambient measurements [3]. Both methods have advantages and shortcomings.

The methods that are based on disturbances can be very accurate [4] provided that the on-set of the disturbance is correctly detected [5]–[8]. This can be challenging in low-inertia power systems, which show a “rich” dynamical behavior [9]. Moreover, the estimation cannot be performed continuously, but only following disturbances [10] [11]. Methods based on signal injection must inject active power of adequate

magnitude and require the installation of specific equipment or the modification of pre-existing controllers [12].

The methods that utilize ambient measurements are conceptually more challenging than those based on disturbances. The main advantage of these methods is that they employ measurements obtained in normal operating conditions and hence the estimation can be performed in a continuous fashion. The starting point is to build the dynamical model of the system, which can be either complete or reduced to a small number of coherent areas [13]. Then, the values of the parameters and of the observable state variables are fit to available measurements.

In this second group, we cite, for example, [14], where the authors obtain the fitting based on a robust Kalman filter. In [15] such a task is performed using a closed-loop identification method. In [16]–[18] inertia estimation is performed by observing the step response of the reduced-order model obtained from the full state-space model describing the grid, which is, in turn, obtained through parameter identification using ambient measurements. In [19] the power grid is reduced to a two-machine system and then the system inertia is estimated using inter-area oscillation modes. The approach proposed in [20] estimates the inertia constants of each generator by applying the regression theorem to a set of Ornstein-Uhlenbeck (OU) processes. The method utilizes the covariance and correlation matrices of the state variables to estimate the state matrix of the system. Then, the inertia constants are obtained solving a least-square problem. The main limitation of [20] is the assumption that the relationship between the active power variations of synchronous machines and the voltage angle variations, as well as the active and reactive power variations of converter-interfaced generators are linear.

### C. Contribution

The approach proposed in this work falls in the group of methods that use ambient measurements. We propose to exploit the *colored noise* due to random fluctuations of the power consumption of the loads and their impact on bus voltages, line currents, and power flows across different areas of a power system. Then we define analytically the statistical properties of the colored noise of these electrical quantities as functions of the system parameters and of the inertia present in the system. Finally, we utilize the variance of the electrical measurements to minimize a non-linear least-squares cost function with respect to the equivalent inertia constants as well as the equivalent damping coefficients of the generators, either synchronous or power-electronic based, that are connected to the grid. The solution is the sought value of the inertia constant or of the damping coefficient that best fit the measurements and that satisfy the grid constraints.

F. Bizzarri is with Politecnico di Milano, DEIB, p.zza Leonardo da Vinci, no. 32, 20133 Milano, Italy and also with the Advanced Research Center on Electronic Systems for Information and Communication Technologies E. De Castro (ARCES), University of Bologna, 41026 Bologna, Italy. (e-mail: federico.bizzarri@polimi.it).

D. del Giudice, S. Grillo, D. Linaro, and A. Brambilla are with Politecnico di Milano, DEIB, p.zza Leonardo da Vinci, no. 32, Milano, 20133, Italy. (e-mails: {davide.delgiudice, samuele.grillo, daniele.linaro, angelo.brambilla}@polimi.it).

F. Milano is with School of Electrical & Electronic Eng., University College Dublin, Belfield Campus, Dublin, D04V1W8, Ireland. (e-mail: federico.milano@ucd.ie).

#### D. Organization

The remainder of the paper is structured as follows. Section II gives the theoretical mathematical background of power systems' modeling and in Section III the mathematical model is enriched with the introduction of noise injections to the power system, being this stage instrumental to model load variability and perform the estimation. Section IV presents the proposed estimation procedure. Then the proposed method is validated through numerical simulations, which are discussed in Section V. This section also discusses the challenges posed by the proposed approach and presents a solution based on a proper filtering of the measurements. Finally, conclusions are drawn in Section VI.

### II. POWER SYSTEM MODEL

The proposed estimation procedure assumes that the generators connected to the grid are synchronous machines and fits the measurements to this model. In this section, we formulate the equations of the system according to this assumption. It is important to note, however, that every simulation is carried out utilizing a full-fledged model representing in detail the dynamical behavior of all generators, either synchronous or non-synchronous, and their controllers.

To describe the dynamics of the power system model (PSM), we consider the following set of differential algebraic equations (DAEs)

$$\begin{aligned} \dot{\delta} &= \Omega(\omega - \omega_0), \\ M\dot{\omega} &= P_m(\omega, x, y) - P_e(\delta, x, v, \theta, y) - D(\omega - \omega_0) \\ T\dot{x} &= \tilde{F}(\delta, \omega, x, v, \theta, y), \\ 0 &= G(\delta, \omega, x, v, \theta, y), \end{aligned} \quad (1)$$

where, assuming that  $M$  is the number of machines, the meaning of symbols in (1) is as follows:

- $\Omega$ : the base synchronous frequency in rad/s;
- $\omega(t) \in \mathbb{R}^M$ : the rotor speeds of the machines;
- $\omega_0 \in \mathbb{R}$ : the reference synchronous frequency;
- $\delta(t) \in \mathbb{R}^M$ : the rotor angles of the machines;
- $M \in \mathbb{R}^{M \times M}$ : a diagonal matrix whose entries model the inertia constants of the machines;
- $x(t) \in \mathbb{R}^N$ : the  $N$  state variables of the PSM ( $\omega$  and  $\delta$  excluded) that can influence the dynamics of the machines, and  $T \in \mathbb{R}^{N \times N}$  is a proper mass matrix;
- $y(t) \in \mathbb{R}^S$ : all the algebraic variables of the PSM but  $v$  and  $\theta$ ;
- $D \in \mathbb{R}^{M \times M}$ : a diagonal matrix whose entries  $d_{jj}$  (for  $j = 1, \dots, M$ ) model the damping factor of the machines;
- $v(t) \in \mathbb{R}^P$  and  $\theta(t) \in \mathbb{R}^P$ : bus voltages and phases, respectively, where  $P$  is the number of buses;
- $P_m(\omega, x, y) \in \mathbb{R}^M$ : the mechanical power regulated by controllers depending on  $\omega$ ,  $x$ , and  $y$ ;
- $P_e(\delta, x, v, \theta, y) \in \mathbb{R}^M$ : the electrical power exchanged by machines;
- $\tilde{F}(\cdot)$  accounts for regulators and other dynamics included in the system; and
- $G(\cdot)$  models algebraic constraints such as lumped models of transmission lines, transformers and static loads.

Equation (1) can be conveniently rewritten as

$$\begin{aligned} \Lambda \dot{\xi} &= \tilde{F}(\xi, \zeta), \\ 0 &= G(\xi, \zeta), \end{aligned} \quad (2)$$

where  $\xi(t) \equiv [\omega, \delta, x]^T$ ,  $\zeta(t) \equiv [v, \theta, y]^T$ , and  $\Lambda$  is a non-singular diagonal matrix.  $\tilde{F}$  and  $G$  are assumed to be continuously differentiable in their definition domain and matrices of their partial derivatives are referred to as  $\tilde{F}_\xi$ ,  $\tilde{F}_\zeta$ ,  $G_\xi$ , and  $G_\zeta$ . As an example,  $\tilde{F}_{\xi_{jk}} = \partial \tilde{F}_j / \partial \xi_k$ , for  $j, k = 1, \dots, 2M + N$ .

The implicit function theorem guarantees that if  $G(\xi^*, \zeta^*) = 0$ , provided that  $G_\zeta(\xi^*, \zeta^*)$  is not singular, a unique and smooth function  $\Gamma: \mathbb{R}^{2M+N} \rightarrow \mathbb{R}^{2P+S}$  exists so that  $\zeta^* = \Gamma(\xi^*)$ . If the conditions of the implicit function theorem are satisfied, (2) can be rewritten as

$$\Lambda \dot{\xi} = \tilde{F}(\xi, \Gamma(\xi)) \equiv F(\xi), \quad (3)$$

the equilibrium points of which, say  $\xi_o$ , satisfy the condition

$$F(\xi_o) = 0, \quad (4)$$

with the Jacobian matrix

$$J(\xi_o) = \Lambda^{-1} F_\xi = \Lambda^{-1} (\tilde{F}_\xi - \tilde{F}_\zeta G_\zeta^{-1} G_\xi) \Big|_{\xi=\xi_o, \zeta=\Gamma(\xi_o)}. \quad (5)$$

### III. INCLUSION OF NOISE

We assume stochastic noise is injected into the PSM as

$$\begin{aligned} \Lambda \dot{\xi} &= \tilde{F}(\xi, \zeta), \\ 0 &= G(\xi, \zeta) + \Xi \eta, \end{aligned} \quad (6)$$

where  $\eta$  is a vector of  $Z$  independent Ornstein-Uhlenbeck (OU) processes [21], and  $\Xi \in \mathbb{R}^{(2P+S) \times Z}$  is a constant matrix.

The OU processes are defined through a set of stochastic differential equations (SDEs), as follows

$$d\eta = -\Upsilon \eta dt + \Sigma dW_t, \quad (7)$$

where the drift  $\Upsilon \in \mathbb{R}^{Z \times Z}$  and diffusion  $\Sigma \in \mathbb{R}^{Z \times Z}$  are diagonal matrices with positive entries,  $W_t \in \mathbb{R}^Z$  is a vector of  $Z$  Wiener processes, and the differentials rather than time derivatives are utilized to account for the idiosyncrasies of the Wiener processes. The OU processes are characterized by a mean-reversion property and show bound standard deviation. Moreover, these processes show a spectrum that is an accurate model of the stochastic variability of power loads [22]–[26]. In (6), we assume that noise injection models the effect of the consumption randomness of  $Z$  loads.

Note that, in (6), the vector of stochastic processes  $\eta$  appears only in the algebraic equations. This is assumed for simplicity but without lack of generality. The interested reader can find for instance in [24] a stochastic PSM model where the noise perturbs both differential and algebraic equations.

We also assume that the action of  $\eta$  can be safely modeled as a small-signal perturbation around an equilibrium point. Hence, the solution of (6) can be written as  $\xi = \xi_o + \xi_\eta$  and  $\zeta = \zeta_o + \zeta_\eta$ , that is, the effects of perturbations are assumed as additive. It is thus possible to linearize (6) around  $\xi_o$  and obtain the random ordinary differential equation [27]

$$\Lambda \dot{\xi}_\eta = F_\xi \xi_\eta - \tilde{F}_\zeta G_\zeta^{-1} \Xi \eta, \quad (8)$$

where the  $F_\xi$ ,  $\tilde{F}_\zeta$ , and  $G_\zeta$  matrices are computed at  $(\xi_o, \zeta_o)$ . The small-signal variations of the algebraic variables are given by

$$\zeta_\eta = -\underbrace{G_\zeta^{-1} [G_\xi | \Xi]}_E \begin{bmatrix} \xi_\eta \\ \eta \end{bmatrix}. \quad (9)$$

Augmenting (8) with (7) allows obtaining the linear SDEs (in narrow sense [21]) governing the overall dynamics of the linearized noisy PSM. Adopting the typical formalism of the SDEs, the complete set of linearized SDEs reads

$$d \begin{bmatrix} \xi_\eta \\ \eta \end{bmatrix} = \underbrace{\begin{bmatrix} \Lambda^{-1} F_\xi & -\Lambda^{-1} \tilde{F}_\zeta G_\zeta^{-1} \Xi \\ 0 & -\Upsilon \end{bmatrix}}_A \begin{bmatrix} \xi_\eta \\ \eta \end{bmatrix} dt + \underbrace{\begin{bmatrix} 0 \\ \Sigma \end{bmatrix}}_B dW_t, \quad (10)$$

The solution of (10) with a normally distributed (or constant) initial condition is a  $(2M + N + Z)$ -dimensional Gaussian stochastic process.

#### IV. PROPOSED TECHNIQUE TO ESTIMATE THE INERTIA

The mean and the covariance matrix of process (10) can be derived by solving two properly defined sets of linear ordinary differential equations (ODEs) [21]. Since (10) is stable under the hypothesis that (3) is stable at  $\xi_o$ , these ODEs reveal that, at steady state, the mean of  $X_t$  is zero, and its  $K_{X_t}$  covariance matrix derives from the solution of the following Lyapunov equation

$$AK_{X_t} + K_{X_t}A^T + BB^T = 0. \quad (11)$$

The diagonal elements of  $K_{X_t}$  are the (steady-state) variances of the components of the  $X_t$  process. In particular, the last  $Z$  diagonal elements can be written as  $\sigma_z^2/(2v_z)$ , for  $z = 1, \dots, Z$ , where  $\sigma_z$  and  $v_z$  are the diagonal elements of  $\Sigma$  and  $\Upsilon$ , respectively. These are the (steady-state) variances of the  $Z$  OU processes  $\eta$ .

According to (9),  $\zeta_\eta$  can be written as a linear combination of the entries of  $X_t$ .  $\zeta_\eta$  is a multidimensional Gaussian process, too. Furthermore, the  $K_{\zeta_\eta}$  covariance matrix of the small-signal algebraic variables is given by [28]

$$K_{\zeta_\eta} = EK_{X_t}E^T. \quad (12)$$

The proposed approach exploits (12) and the fact that  $K_{\zeta_\eta}$ , and hence the variance of the algebraic variables, depends, through  $K_{X_t}$  and  $A$ , on the elements of  $\Lambda$ , a subset of which are the inertia constants of the synchronous machines.

Let us assume one wants to estimate a subset  $\mathcal{M}$  of these inertia constants and let  $\mathcal{Z}$  be a set of measurements of bus voltages and currents flowing through a given number of transmission lines and/or transformers.

The derivations given above show that, if the model and the parameters of the grid are known, it is possible to compute the  $\sigma_{\mathcal{Z}}^2$  variances of the measured quantities, which are the diagonal elements of the  $K_{\zeta_\eta}$  matrix. However, it is also possible to solve an inverse problem, namely, knowing through measurements the variance of the elements of  $\mathcal{Z}$ , one can determine the values of the elements of  $\mathcal{M}$  by minimizing

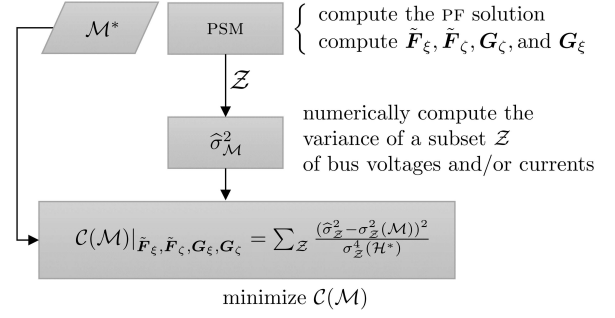


Fig. 1. The flow-diagram of the proposed inertia estimation procedure.

the following non-linear least-squares cost function w.r.t. the elements of  $\mathcal{M}$  (see also Fig. 1):

$$\mathcal{C}(\mathcal{M})|_{\tilde{F}_\xi, \tilde{F}_\zeta, G_\xi, G_\zeta} = \sum_{\mathcal{Z}} \frac{(\hat{\sigma}_{\mathcal{Z}}^2 - \sigma_{\mathcal{Z}}^2(\mathcal{M}))^2}{\sigma_{\mathcal{Z}}^4(\mathcal{M}^*)}, \quad (13)$$

where  $\hat{\sigma}_{\mathcal{Z}}^2$  are the measured values and  $\sigma_{\mathcal{Z}}^2(\mathcal{M}^*)$  are the variances obtained for a reference set of  $\mathcal{M}$  values and are used to normalize the cost function.

We note that the procedure above is *agnostic* w.r.t. to the devices that are connected to the grid. That is, the estimation of the inertia is obtained by fitting the synchronous machine model to the measurements. If there exist non-synchronous devices, such as converter-interfaced generation, their “equivalent” inertia constants can be obtained using (13) regardless of the fact that the converter is set up to be grid forming or grid following. The procedure is also agnostic in terms of the parameters to be estimated, provided that such parameters do have an effect on the frequency variations of the system. In particular, we use this property to estimate the equivalent damping coefficients of the devices, the estimation of which can be obtained by minimizing a cost function for a subset of damping coefficients  $\mathcal{D}$ , in a similar way as for  $\mathcal{M}$  in (13),

$$\mathcal{C}(\mathcal{D})|_{\tilde{F}_\xi, \tilde{F}_\zeta, G_\xi, G_\zeta} = \sum_{\mathcal{Z}} \frac{(\hat{\sigma}_{\mathcal{Z}}^2 - \sigma_{\mathcal{Z}}^2(\mathcal{D}))^2}{\sigma_{\mathcal{Z}}^4(\mathcal{D}^*)}. \quad (14)$$

#### V. CASE STUDY

We use as a benchmark the IEEE 39-bus power system shown in Fig. 2 [29]. This is a simplified model of the transmission system in the New England region in the North-eastern United States and is composed of 10 generators, 34 lines, 19 loads, and 12 transformers. The network models and parameters are those adopted and directly extracted from its DIGSILENT PowerFactory implementation [30] and derived from [31]. Automatic voltage regulators (AVRs), used for the synchronous generators in the IEEE 39-bus power system, are rotating excitation systems of IEEE Type 1 according to [31]. The  $G_1$  generator, which represents the connection of the New England System to the rest of the US and Canadian grid, is modeled with a constant excitation [31], viz. there is no AVR connected to  $G_1$ . Governors (GOVs) are considered as IEEE Type G1 (steam turbine) for  $G_2$ – $G_9$ , and IEEE Type G3 (hydro turbine) for  $G_{10}$ . Finally, in Table I we report the value of

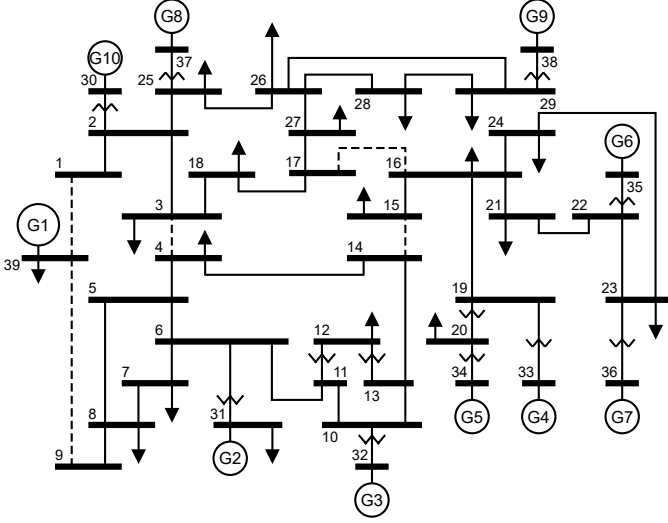


Fig. 2. The single-line diagram of the IEEE 39-bus power system.

inertia constants of the 10 generators and the corresponding power rating.

The active power consumption of each of the  $Z = 19$  loads is altered by one of the  $\eta_z(t)$  OU processes ( $z = 1, \dots, Z$ ) in (10), which has zero mean, and variance  $\sigma_z^2/(2v_z)$ . All loads are assumed to incorporate stochastic power fluctuations [24]

$$L_z(t) = \eta_z(t) P_{L0_z} \left( \frac{|v_z(t)|}{V_{0_z}} \right)^\gamma, \quad (15)$$

where (for  $z = 1, \dots, Z$ )  $P_{L0_z}$  is the nominal active power of the load,  $V_{0_z}$  is the load voltage rating,  $v_z(t)$  is the bus voltage at which the load is connected and  $\gamma$  governs the dependence of the load on bus voltage. In the simulation below, we assume  $v_z = 0.5$  and  $\sigma_z$  is defined in such a way that the standard deviation of  $\eta_z(t)$  is 5% of  $P_{L0}$ . The zero mean implies that stochastic load power fluctuations do not perturb, on average, the operating point of the system. Furthermore, we assumed  $\gamma = 0$ .

To carry out the simulations discussed below, the numerical integration of the multi-dimensional OU process in (6) was based on the numerical scheme proposed by Gillespie in [32]. Furthermore, the second-order trapezoidal implicit weak scheme for stochastic differential equations with colored noise, available in the simulator PAN [33], [34], was adopted [35].

#### A. Conventional Power System

The objective of the first scenario considered in this case study is to estimate the inertia constants of the 10 generators of

TABLE I  
SYNCHRONOUS GENERATORS  $H$  AND  $P_{\text{RAT}}$

Generator	$H$ [s]	$P_{\text{RAT}}$ [MW]	Generator	$H$ [s]	$P_{\text{RAT}}$ [MW]
$G_1$	5.00	10000	$G_6$	4.35	800
$G_2$	4.33	700	$G_7$	3.77	700
$G_3$	4.47	800	$G_8$	3.47	700
$G_4$	3.57	800	$G_9$	3.45	1000
$G_5$	4.33	600	$G_{10}$	4.20	1000

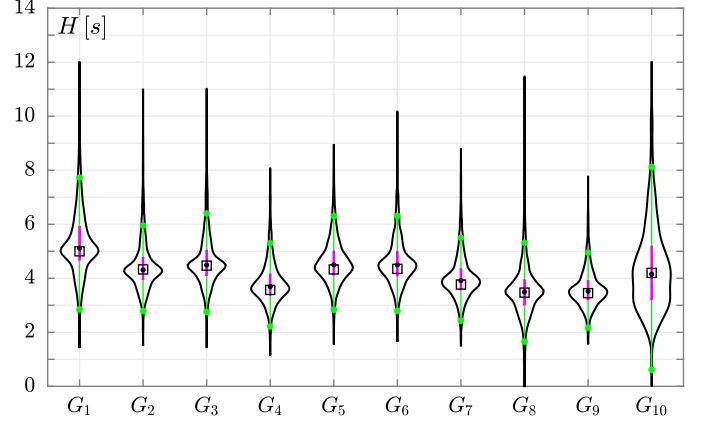


Fig. 3. The black solid circle marker correspond to the median value of the optimization results, whereas the empty square marker represents the nominal value of the inertia constants. The magenta bars represents the IQR, viz. the spread difference between the 75<sup>th</sup> and 25<sup>th</sup> percentiles of the data. The green solid circle markers represent the upper adjacent value (i.e., the largest observation that is less than or equal to the third quartile plus  $1.5 \times \text{IQR}$ ) and the lower adjacent value (i.e., the smallest observation that is greater than or equal to the first quartile minus  $1.5 \times \text{IQR}$ ). Time window: 15 min. Optimization performed on the unfiltered currents.

the IEEE 39-bus system across a time period spanning one day. The target is to obtain an estimation of the inertia constants every 15 min (estimation window) of the working day. To this end, we compute the variance of the currents flowing through the generators, using a 15 min-long moving window. The values of variance are the elements of the  $\mathcal{M}$  set introduced in Sec. IV. The sampling period is 25 ms, i.e., a sampling rate of 40 Hz. We also assume that the state matrix  $\mathbf{A}$  of the system is constant, i.e., that the parameters of the IEEE 39-bus system do not vary during the simulation. This assumption simplifies the analysis but is not a binding requirement of the proposed procedure. If the operating point and/or the topology of the grid change, one just needs to update matrix  $\mathbf{A}$ .

The inertia constants were obtained with the MATLAB Global Optimization Toolbox and the `fgoalattain` function. The search interval of the optimization procedure was lower-bounded to zero. An optimization problem is solved every 15 min of simulated time by collecting 1920 estimates per synchronous generator. The violin plots<sup>1</sup> in Fig. 4 (one for each generator) summarize the obtained results. The median of the estimated value of the inertia constants (black solid dots in Fig. 3) are in good agreement with the corresponding nominal values (empty squared markers in Fig. 3) listed in Table I. Despite the amplitude of the interquartile range (IQR) intervals (magenta vertical bars in Fig. 3) are reasonably narrow, the upper and lower adjacent values (green solid dots in Fig. 3) are quite far from the median values, and the same holds for the tails of the distribution of the estimated values.

The quality of the results can be improved by filtering the considered currents before computing their moving variance. This is done by resorting to a steep bandpass filter acting from

<sup>1</sup>A violin plot is a combination of a box plot and a kernel density plot. Specifically, it starts with a box plot and then adds a rotated kernel density plot to each side of the box plot.

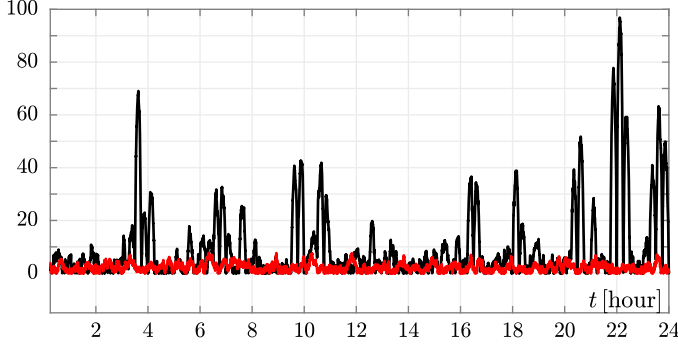


Fig. 4. The percentage relative error of the moving variance of the  $i_8$  current, calculated over a sliding window of 15 min, with respect to the steady-state variance of  $i_8$ . The black and the red curve refer to the unfiltered and filtered case, respectively.

0.1 Hz to 1.5 Hz. This bandwidth was chosen to remove the low frequency contribution of the OU process. This is done since these components account for the very slow fluctuations of the currents that heavily affect the trend of their moving variance w.r.t. the steady-state values of the variance itself. The effect of this filter is shown in Fig. 4 for the  $i_8$  current (i.e., the current flowing through  $G_8$ ) in terms of the absolute value of the relative percentage error between the moving variance and its steady-state value over 24 h in one realization of the 20 trials. In particular, the black and red curves refer to the unfiltered and the filtered case, respectively, and the improvement over the unfiltered case is evident.

The state equations governing the dynamics of the filters were added to the set of ODEs reported in (3) and this allowed to derive the steady-state variance of the filters output solving (11). The inertia constants of the IEEE 39-bus generators was estimated from the filtered currents and the results are reported in Fig. 5. The effect of this signal processing is a significant reduction of the amplitude of the interval spanned by the upper and lower adjacent values thus guaranteeing a more reliable estimate of the inertia constants.

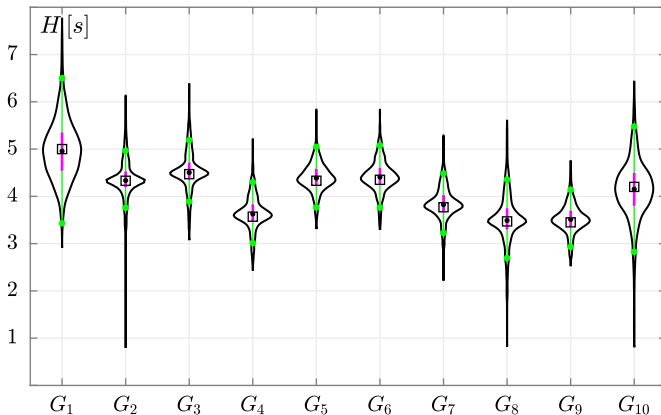


Fig. 5. Time window: 15 min. Optimization performed on the filtered currents. Note the different scale of the vertical axes w.r.t. Fig. 3.

These results illustrate well that the proposed approach accurately estimates the inertia constants of the ten synchronous generators of the system.

### B. Inclusion of Grid-Forming Converters

This section illustrates the behavior of the proposed estimation technique for a scenario where the IEEE 39-bus system includes a variable generation/load profile and grid-forming converters. These devices are assumed to mimic the behavior of synchronous machines and are thus expected to provide a *virtual* inertia to the system. The objective of this section is twofold: (i) showing that the proposed inertia estimation approach works correctly under variable generation/load conditions and (ii) illustrating the ability of the proposed estimation technique to capture the effect of grid-forming converters.

With this aim, we first modified the IEEE 39-bus system by mimicking a typical daily variation of the loads. To do so, we multiplied the power absorbed by the loads and the (active) power generated by the synchronous machines by a coefficient  $\lambda$ . To alter the nominal value of the power loads,  $\lambda$  was varied continuously in time according to the profile shown in the upper panel of Fig. 6. To update the set point of the generators, this profile was sampled every 15 min. The effect of energy production by three (aggregated) solar plants connected to bus<sub>8</sub>, bus<sub>24</sub>, and bus<sub>27</sub> (one in each significant area of the network, see Fig. 2) was emulated by reducing the absorbed active power of the loads connected at those buses. Load power was decreased by the same active power supplied by those (aggregated) solar plants (each one supplying one third of the electrical power reported in the lower panel of Fig. 6). To balance generation the power supplied by these plants was subtracted from the power of synchronous generators. In particular, the active power supplied by  $G_3$ ,  $G_7$ , and  $G_8$  was varied in proportion to their power ratings.

The set point of the generators is updated every 15 min. The power rating of each one of the virtual synchronous generators is 100 MW. Finally, we assume that the solar power plants provide synthetic inertia through the controllers of their inverters only from 8:15 am to 5:30 pm. In this period, the solar power plants are regulated to provide a total virtual inertia equivalent to  $H = 10$  s.

Results are shown in Fig. 7, using again violin plots. The left panel refers to the time interval in which the solar plants are not connected and thus the inertia constants of the grid-forming converters is zero. The right panel corresponds to the 8:15 am – 5:30 pm time interval. The estimation is accurate even though we utilized current measurements of branches far away from the buses of the solar power plants, i.e., the branches indicated with dashed lines in Fig. 2.

Moreover we observe the birth of additional “swing equation” modes due to the presence of this kind of the virtual synchronous generators [36]. These, in fact, induce inter-area oscillations that are clearly identified by peaks in the frequency responses by frequency scan. Modifying the inertia constant of these elements changes significantly the variance of the measured electrical quantities and, thus, helps increasing the accuracy of the proposed technique.

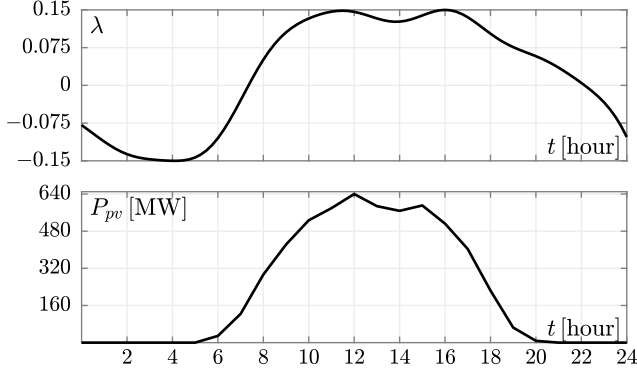


Fig. 6. Upper panel: time evolution of the  $\lambda$  coefficient used to overload the IEEE 39-bus system. Lower panel: the overall active power supplied by the solar plants that were added to the IEEE 39-bus system.

Figure 8 shows the estimation of the inertia of the system across the full day of measurements. This illustrates the effectiveness of the proposed technique to *continuously* estimate the inertia by stochastic fluctuations. In Fig. 8, the black traces are single trials while the red one is the median value over 50 trials. All realisations give accurate results with only a few time instants being affected by a relatively higher error.

### C. Inclusion of Grid-Following (GFL) Converters

In the third and last scenario, we discuss the effect of the frequency droop control of grid-following converters on the estimation of the inertia with the proposed technique. As is well-known, the frequency droop control of the converter is equivalent to a second order model, and is thus similar to that of synchronous machines, except for the fact that it shows a large damping and approximately zero inertia [37]. In this scenario, thus, we repeat the simulations with the modified IEEE 39-bus system with inclusion of the same solar power plants considered in the previous section. However, we

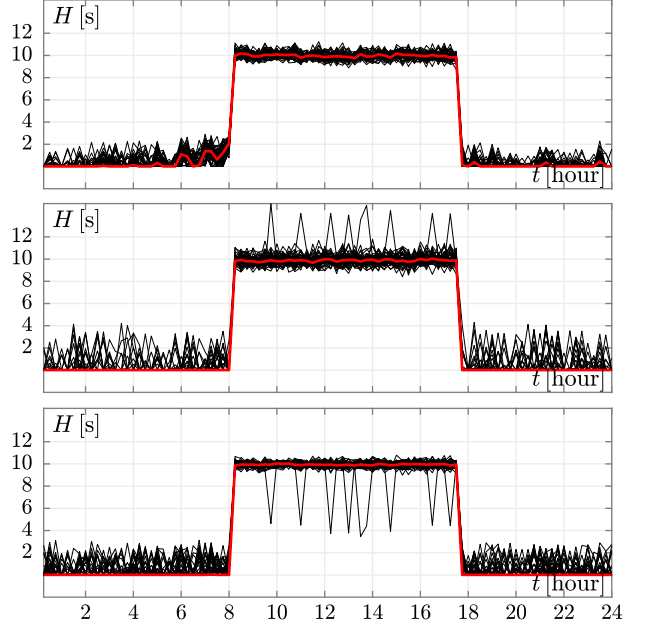


Fig. 8. The inertia constants of the grid-forming converters GFM<sub>1</sub>, GFM<sub>2</sub>, and GFM<sub>3</sub> (from the upper to the lower panel) were set to 10 s from 8:15 am to 5:30 pm. The results of the 50 estimation procedures are depicted in black. In red we report the median value computed every 15 min over the 50 trials.

assume that these plants are now equipped with conventional frequency droop controllers.

Table II shows that the estimation of the damping/droop and of the inertia are strongly correlated. An increase in the droop coefficients of the frequency controllers leads to a lower inertia constant estimation. This result had to be expected as a lower droop makes the response of the controller slower and thus its time scale tends to overlap with that of the inertial response. The estimation of the inertia constant and of the damping coefficient are performed independently, since two separate least-squares problems are solved: one fits the inertia constant and a second one fits the damping coefficient.

The main conclusion that can be drawn from the results shown in Table II is that the value of the inertia constant alone is not sufficient to define the ability of a device to regulate the frequency. If only the inertia constant is estimated, in fact, one would conclude that the case with lower droop coefficient is the one with lower frequency containment, which is not. On the other hand, if both parameters, namely inertia and damping, are estimated, then one can conclude, correctly, that the system with higher droop provides “more” fast frequency control than inertial response. On the other hand, lower droop values increase the ability of the system to have an inertial response but lead, as expected, to a lower capability of providing a service as fast frequency controllers.

## VI. CONCLUSIONS

This work proposes a technique to estimate the inertia based on the variance of measurements. The technique assumes a given structure of the system and the dynamics of the generators and fits, by solving a least-squares problem, this

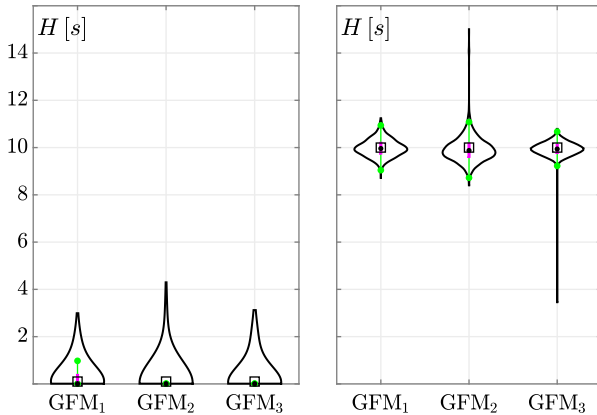


Fig. 7. The inertia constants of the grid-forming converters GFM<sub>1</sub>, GFM<sub>2</sub>, and GFM<sub>3</sub> were set to 10 s from 8:15 am to 5:30 pm. Left and right panels refer to the low- and high-inertia cases, respectively. The time window is 15 min.



TABLE II

ESTIMATION OF THE EQUIVALENT INERTIA AND OF THE DAMPING/DROOP FOR THE IEEE 39-BUS SYSTEM WITH INCLUSION OF GRID-FOLLOWING CONVERTERS.

Device	droop = 2		droop = 10	
	$H_{eq}$ [s]	$D_{eq}$ [pu]	$H_{eq}$ [s]	$D_{eq}$ [pu]
GFL <sub>1</sub>	0.64	3.29	0.40	8.65
GFL <sub>2</sub>	0.60	3.13	0.37	7.97
GFL <sub>3</sub>	0.56	3.93	0.34	10.57

model to the measurements. Simulation results show that the proposed technique, given a proper filtering of the measurements, is accurate and can take into account both conventional and virtual synchronous machines, as well as the effect of frequency droop controller. However, the correct interpretation of the effect of droop controllers is consistent only if also the damping/droop coefficients are estimated, which the proposed technique duly allows to obtain.

In particular, we believe that the proposed technique can be useful to properly reward the frequency support provided by non-synchronous devices. In turn, we recommend that the reward should be evaluated based on the *effect* that the controllers of these devices have on the system, not on the actual implementation of the control itself.

Future work will focus on further investigating the theoretical and practical aspects of the proposed technique. For example, relevant questions are how to improve the accuracy of the estimated inertia constants through a proper choice of the set of measurements and of the filtering of the measurements.

## REFERENCES

- [1] A. Ulbig, T. S. Borsche, and G. Andersson, "Impact of low rotational inertia on power system stability and operation," *IFAC Proceedings Volumes*, vol. 47, no. 3, pp. 7290–7297, 2014, 19th IFAC World Congress. [Online]. Available: <https://www.sciencedirect.com/science/article/pii/S1474667016427618>
- [2] F. Milano, F. Dörfler, G. Hug, D. J. Hill, and G. Verbič, "Foundations and challenges of low-inertia systems (invited paper)," in *2018 Power Systems Computation Conference (PSCC)*, 2018, pp. 1–25.
- [3] B. Tan, J. Zhao, M. Netto, V. Krishnan, V. Terzija, and Y. Zhang, "Power system inertia estimation: Review of methods and the impacts of converter-interfaced generations," *Int. J. Electr. Power Energy Syst.*, vol. 134, no. 107362, 2022.
- [4] U. Tamrakar, N. Guruswamy, N. Bhujel, F. Wilches-Bernal, T. M. Hansen, and R. Tonkoski, "Inertia estimation in power systems using energy storage and system identification techniques," in *2020 International Symposium on Power Electronics, Electrical Drives, Automation and Motion (SPEEDAM)*, 2020, pp. 577–582.
- [5] P. Wall and V. Terzija, "Simultaneous Estimation of the Time of Disturbance and Inertia in Power Systems," *IEEE Trans. Power Del.*, vol. 29, no. 4, pp. 2018–2031, Aug. 2014.
- [6] D. Zografos, M. Ghandhari, and R. Eriksson, "Power system inertia estimation: Utilization of frequency and voltage response after a disturbance," *Electr. Pow. Syst. Res.*, vol. 161, pp. 52–60, 2018.
- [7] P. M. Ashton, C. S. Saunders, G. A. Taylor, A. M. Carter, and M. E. Bradley, "Inertia Estimation of the GB Power System Using Synchrophasor Measurements," *IEEE Trans. Power Syst.*, vol. 30, no. 2, pp. 701–709, Mar. 2015.
- [8] D. del Giudice and S. Grillo, "Analysis of the Sensitivity of Extended Kalman Filter-Based Inertia Estimation Method to the Assumed Time of Disturbance," *Energies*, vol. 12, no. 483, 2019.
- [9] E. Heylen, F. Teng, and G. Strbac, "Challenges and opportunities of inertia estimation and forecasting in low-inertia power systems," *Renew. Sustain. Energy Rev.*, vol. 147, no. 111176, 2021.
- [10] R. K. Panda, A. Mohapatra, and S. C. Srivastava, "Online Estimation of System Inertia in a Power Network Utilizing Synchrophasor Measurements," *IEEE Trans. Power Syst.*, vol. 35, no. 4, pp. 3122–3132, Jul. 2020.
- [11] G. Cai, B. Wang, D. Yang, Z. Sun, and L. Wang, "Inertia Estimation Based on Observed Electromechanical Oscillation Response for Power Systems," *IEEE Trans. Power Syst.*, vol. 34, no. 6, pp. 4291–4299, Nov. 2019.
- [12] J. Zhang and H. Xu, "Online Identification of Power System Equivalent Inertia Constant," *IEEE Trans. Ind. Electron.*, vol. 64, no. 10, pp. 8098–8107, Oct. 2017.
- [13] G. R. Moraes, F. Pozzi, V. Ilea, A. Berizzi, E. M. Carlini, G. Giannuzzi, and R. Zottini, "Measurement-based inertia estimation method considering system reduction strategies and dynamic equivalents," in *2019 IEEE Milan PowerTech*, 2019, pp. 1–6.
- [14] J. Zhao, Y. Tang, and V. Terzija, "Robust Online Estimation of Power System Center of Inertia Frequency," *IEEE Trans. Power Syst.*, vol. 34, no. 1, pp. 821–825, Jan. 2019.
- [15] J. Zhang and H. Xu, "Online Identification of Power System Equivalent Inertia Constant," *IEEE Trans. Ind. Electron.*, vol. 64, no. 10, pp. 8098–8107, Oct. 2017.
- [16] F. Zeng, J. Zhang, G. Chen, Z. Wu, S. Huang, and Y. Liang, "Online estimation of power system inertia constant under normal operating conditions," *IEEE Access*, vol. 8, pp. 101 426–101 436, 2020.
- [17] V. Baruzzi, M. Lodi, A. Oliveri, and M. Storace, "Analysis and improvement of an algorithm for the online inertia estimation in power grids with RES," in *2021 IEEE International Symposium on Circuits and Systems (ISCAS)*. IEEE, 2021, pp. 1–5.
- [18] —, "Estimation of inertia in power grids with turbine governors," in *2022 IEEE International Symposium on Circuits and Systems (ISCAS)*. IEEE, 2022, pp. 1–5.
- [19] D. Yang, B. Wang, J. Ma, Z. Chen, G. Cai, Z. Sun, and L. Wang, "Ambient-data-driven modal-identification-based approach to estimate the inertia of an interconnected power system," *IEEE Access*, vol. 8, pp. 118 799–118 807, 2020.
- [20] J. Guo, X. Wang, and B.-T. Ooi, "Online purely data-driven estimation of inertia and center-of-inertia frequency for power systems with vsc-interfaced energy sources," *Int. J. Electr. Power Energy Syst.*, vol. 137, no. 107643, 2022.
- [21] L. Arnold, *Stochastic differential equations*, ser. A Wiley-Interscience publication. Wiley, 1974.
- [22] R. H. Hirpara and S. N. Sharma, "An Ornstein-Uhlenbeck process-driven power system dynamics," *IFAC-PapersOnLine*, vol. 48, no. 30, pp. 409–414, 2015, 9th IFAC Symposium on Control of Power and Energy Systems CPES 2015.
- [23] C. Nwankpa and S. Shahidehpour, "Colored noise modelling in the reliability evaluation of electric power systems," *Appl. Math. Model.*, vol. 14, no. 7, pp. 338–351, 1990.
- [24] F. Milano and R. Zárate-Miñano, "A systematic method to model power systems as stochastic differential algebraic equations," *IEEE Trans. Power Syst.*, vol. 28, no. 4, pp. 4537–4544, Nov. 2013.
- [25] C. Roberts, E. M. Stewart, and F. Milano, "Validation of the ornstein-uhlenbeck process for load modeling based on  $\mu$ PMU measurements," in *2016 Power Systems Computation Conference (PSCC)*, 2016, pp. 1–7.
- [26] H. Hua, Y. Qin, C. Hao, and J. Cao, "Stochastic Optimal Control for Energy Internet: A Bottom-Up Energy Management Approach," *IEEE Trans. Ind. Informat.*, vol. 15, no. 3, pp. 1788–1797, Mar. 2019.
- [27] H. Xiaoying and P. Kloeden, *Random Ordinary Differential Equations and Their Numerical Solution*, ser. Probability Theory and Stochastic Modelling. Springer Singapore, 2017, no. 85.
- [28] S. Provost and A. Mathai, *Quadratic Forms in Random Variables: Theory and Applications*, ser. Statistics: textbooks and monographs. Marcel Dekker, 1992.
- [29] T. Athay, R. Podmore, and S. Virmani, "A Practical Method for the Direct Analysis of Transient Stability," *IEEE Trans. Power App. Syst.*, vol. PAS-98, no. 2, pp. 573–584, Mar./Apr. 1979.
- [30] DlgSILENT PowerFactory, "39 Bus New England System," DlgSILENT GmbH, Tech. Rep., 2014, (downloaded in April 2022). [Online]. Available: <https://qdoc.tips/39-bus-new-england-system-pdf-free.html>
- [31] M. A. Pai, *Energy Function Analysis for Power System Stability*, ser. Kluwer International Series in Engineering and Computer Science, Power Electronics & Power Systems. Boston: Kluwer Academic Publishers, 1989.
- [32] D. T. Gillespie, "Exact numerical simulation of the ornstein-uhlenbeck process and its integral," *Phys. Rev. E*, vol. 54, pp. 2084–2091, Aug 1996.

- [33] F. Bizzarri and A. Brambilla, "PAN and MPanSuite: Simulation vehicles towards the analysis and design of heterogeneous mixed electrical systems," in *NGCAS, Genova, Italy*, Sept. 2017, pp. 1–4.
- [34] F. Bizzarri, A. Brambilla, G. Storti Gajani, and S. Banerjee, "Simulation of real world circuits: Extending conventional analysis methods to circuits described by heterogeneous languages," *IEEE Circuits Syst. Mag.*, vol. 14, no. 4, pp. 51–70, 2014.
- [35] G. N. Milshtein and M. V. Tret'yakov, "Numerical solution of differential equations with colored noise," *Journal of Statistical Physics*, vol. 77, no. 3, pp. 691–715, 1994.
- [36] S. Hadavi, S. P. Me, B. Bahrani, M. Fard, and A. Zadeh, "Virtual synchronous generator versus synchronous condensers: An electromagnetic transient simulation-based comparison," *CIGRE Science and Engineering*, vol. 2022, no. 24, 2022.
- [37] S. D'Arco and J. A. Suul, "Equivalence of Virtual Synchronous Machines and Frequency-Droops for Converter-Based MicroGrids," *IEEE Trans. Smart Grid*, vol. 5, no. 1, pp. 394–395, Jan. 2014.